KINEMATICS OF t-CHANNEL AND PHOTON RADIATION PROCESSES IN carlomat*

Karol Kołodziej

Institute of Physics, University of Silesia
75 Pułku Piechoty 1, 41-500 Chorzów, Poland
karol.kolodziej@us.edu.pl

(Received October 28, 2019)

The automatic generation of multichannel Monte Carlo phase-space integration routines of carlomat, which up to now took into account only mappings of $\sim 1/s$ or Breit–Wigner behaviour of the s-channel diagrams, is being supplemented with the parameterizations which map away the t-channel, soft and collinear photon or gluon emission. In order to improve numerical stability, the quadruple precision versions of the routines for computation of the helicity amplitudes and phase-space parameterizations have been written and calls to them are being implemented in the code generation part of the program.

DOI:10.5506/APhysPolB.50.1971

1. Motivation

Higher energies and higher luminosity of the current and future colliders, such as HL-LHC [1], HE-LHC [2], ILC [3], CLIC [4], CEPC [5] or FCC [6], pose a challenge not only for experimenters but for theoreticians, too. Higher luminosity calls for higher precision of the Standard Model (SM), or beyond SM, predictions, including radiative corrections, while the increasing energy of initial beams allows to observe reactions with a few heavy particles at a time. These heavy particles almost immediately decay leading to the hard scattering reactions with several, *e.g.* 6, 7, 8, or even more particles in the final state. Therefore, theoretical predictions for such multi-particle reactions, which receive contributions typically from dozens of thousands of the Feynman diagrams already at the leading order (LO), are needed. This obviously calls for a full automation of the cross-section calculation.

* Presented at the XLIII International Conference of Theoretical Physics "Matter to the Deepest", Chorzów, Poland, September 1–6, 2019.

The automation can also be useful in the low-energy regime, for example, if one wants to determine hadronic contributions to the vacuum polarization, which are necessary in order to obtain precise SM predictions for the muon anomaly or for the electromagnetic coupling at the Z peak, $\alpha(M_Z)$. The latter is needed to predict, *e.g.* the W boson mass and the electroweak mixing parameter $\sin^2\theta_W$. Below the J/ψ production threshold, the hadronic contributions to the vacuum polarization cannot be calculated perturbatively, but they can be derived, with the help of dispersion relations, from the energy dependence of the cross section of e^+e^- annihilation into hadrons, which must be measured either by the initial beam energy scan or with the use of a radiative return method, and compared with predictions of a Monte Carlo program, as *e.g.* PHOKHARA [7]. In the region from 1.2 to 2.0 GeV, more than 30 exclusive channels must be measured. If this is done with the radiative return method, as in KLOE, BaBar and BES, the predictions must also include radiation of photons, both from the initial (ISR) and final (FSR) state. Production of hadrons at low energies, as well as the photon radiation off them, is usually described in the framework of some effective model, as *e.g.* Hidden Local Symmetry (HLS) model, which includes quite a number of interaction vertices and mixing terms. Because of that, the number of Feynman diagrams for such radiative hadroproduction reactions may become quite big, see *e.g.* [8].

Multi-particle reactions can be handled with several publicly available multipurpose Monte Carlo (MC) generators, as *e.g.* HELAC/PHEGAS [9], AMAGIC++/Sherpa [10], O'Mega/Whizard [11], MadGraph/MadEvent [12], ALPGEN [13], CompHEP/CalcHEP [14], Comix [15], or carlomat [16].

2. Phase-space integration in carlomat

Consider a multi particle reaction of the form of

$$1 + 2 \to 3 + 4 + \ldots + n \tag{1}$$

with the maximum of $n = 12$, as implemented in carlomat [16]. The true challenge in calculation of the cross section of (1) is not the matrix element, but generation of the efficient multichannel MC routine for the phase-space integration. The standard phase-space integration element of reaction (1)

$$\mathrm{d}^{3n_\mathrm{f}-4}\mathrm{Lips} = (2\pi)^4\delta^{(4)}\left(p_1 + p_2 - \sum_{i=3}^{n} p_i\right)\prod_{i=3}^{n}\frac{\mathrm{d}p_i^3}{(2\pi)^3 2E_i} \tag{2}$$

with $n_\mathrm{f} = n-2$, is reparameterized in the following way. The set of final-state particles $\{3, 4, \ldots, n\}$ is divided into two subsets, dependent on a topology

of the diagram. Denote the four momenta of each subset by q_{i_1} and q_{i_2}, respectively, and make use of the identity

$$\int \mathrm{d}s_i \int \frac{\mathrm{d}^3 q_i}{2E_i}\, \delta^{(4)}\left(q_i - q_{i_1} - q_{i_2}\right) = 1\,, \qquad E_i^2 = s_i + \vec{q}_i^{\,2}\,. \tag{3}$$

By doing so consecutively, Eq. (2) is brought into the following form:

$$\mathrm{d}^{3n_\mathrm{f}-4}\mathrm{Lips} = (2\pi)^{4-3n_\mathrm{f}} \mathrm{d}l_0 \mathrm{d}l_1 \ldots \mathrm{d}l_{n-4} \mathrm{d}s_1 \mathrm{d}s_2 \ldots \mathrm{d}s_{n-4}\,, \tag{4}$$

where invariants s_i, $i = 0, 1, \ldots, n-4$, are defined as $s_i = \left(q_{i_1} + q_{i_2}\right)^2$ and $s_0 = \left(q_{0_1} + q_{0_2}\right)^2 = (p_1 + p_2)^2 = s$, and 2-particle phase-space elements $\mathrm{d}l_i$ are given by

$$\mathrm{d}l_i = \frac{|\vec{q}_{i_1}|}{4\sqrt{s_i}} \mathrm{d}\Omega_i\,, \tag{5}$$

with Ω_i being the solid angle of momentum $\vec{q}_{i_1}$ in the relative centre-of-mass system (c.m.s.), $\vec{q}_{i_1} + \vec{q}_{i_2} = \vec{0}$.

Invariants s_i of Eq. (4) are randomly generated within their physical limits, $s_i^{\min}$ and $s_i^{\max}$, which are automatically deduced from a topology of the Feynman diagram. They are generated either according to the uniform distribution or, if wanted, mappings of the Breit–Wigner shape of the propagators of unstable particles and $\sim 1/s$ behaviour of the propagators of massless particles are performed. An option is included in the program that allows to turn on the mapping if the particle decays into 2, 3, 4, ... on-shell particles. Different phase-space parameterizations obtained in this way can be used for testing purposes.

Denote i^{th} of N different phase-space parameterizations generated by the program as

$$f_i(x) = \mathrm{Lips}_i\,(x)\,, \qquad i = 1, \ldots, N\,, \tag{6}$$

where $x = (x_1, \ldots, x_{3n_\mathrm{f}-4})$ are random arguments, $x_i \in [0, 1]$. It must satisfy the normalization condition

$$\int_0^1 \mathrm{d}x^{3n_\mathrm{f}-4} f_i(x) = \mathrm{vol}(\mathrm{Lips})\,. \tag{7}$$

All the parameterizations $f_i(x)$ are then automatically combined into a single multichannel probability distribution

$$f(x) = \sum_{i=1}^{N} a_i f_i(x)\,, \tag{8}$$

with non-negative weights a_i, $i = 1, \ldots, N$, satisfying the condition

$$\sum_{i=1}^{N} a_i = 1 \qquad \Leftrightarrow \qquad \int_0^1 \mathrm{d}x^{3n_\mathrm{f}-4} f(x) = \mathrm{vol(Lips)}\,. \tag{9}$$

The actual MC integration is performed with the random numbers generated according to the probability distribution $f(x)$ of Eq. (8).

The MC integration in carlomat can be performed iteratively. First, the integral is sampled N times with a rather small number of calls to the integrand, each time with a different phase-space parameterization $f_i(x)$, but equal weights $a_i = 1/N$ of Eq. (8), and the resulting cross section σ_i. Then new weights calculated according to the following formula:

$$a_i = \sigma_i / \sum_{j=1}^{N} \sigma_j \tag{10}$$

are used in the first iteration of the integral. Weights a_i are calculated anew according to Eq. (10) after each consecutive iteration and substituted in distribution $f(x)$ of Eq. (8) with which the next iteration is calculated. This means that channels with small weights a_i are chosen with low probability and will have either small or zero weights in all subsequent iterations.

As all the automatically generated kinematical channels were parameterized according to Eq. (4), the multichannel MC phase-space integration routine of carlomat was up to now adequate basically only for reactions dominated by the s-channel diagrams. What if the t-channel Feynman diagrams become relevant, or if we have to do with a photon/gluon radiation with a soft photon/gluon, or collinear singularity? The question is addressed in Sections 3 and 4.

3. t-channel singularity

Consider the reaction of the following form:

$$e^+(p_1) + e^-(p_2) \to e^+(p_3) + e^-(p_4) + 5 + \ldots + n\,. \tag{11}$$

It receives contributions, among others, from the Feynman diagrams of the form depicted in Fig. 1. Using identity (3), we parameterize the phase-space integration element in the following way:

$$\begin{aligned} \mathrm{d}^{3n_\mathrm{f}-4}\mathrm{Lips} \;=\; & (2\pi)^{4-3n_\mathrm{f}} \mathrm{d}s' \delta^{(4)}\left(p_1 + p_2 - p_3 - p_4 - p'\right) \frac{\mathrm{d}p_3^3}{2E_3} \frac{\mathrm{d}p_4^3}{2E_4} \frac{\mathrm{d}p'^3}{2E'} \\ & \times \delta^{(4)}\left(p' - \sum_{i=5}^{n} p_i\right) \prod_{i=5}^{n} \frac{\mathrm{d}p_i^3}{2E_i}\,, \end{aligned} \tag{12}$$

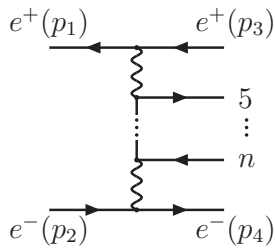

Fig. 1. Feynman diagram of reaction (11) containing double t-channel singularity.

with $E' = \sqrt{s' + \vec{p}'^2}$. The right-hand side (r.h.s.) of Eq. (12) is a convolution of the 3- and $(n_\mathrm{f} - 2)$-particle phase-space elements defined as follows:

$$\mathrm{d}PS_3\left(s, m_3^2, m_4^2, s'\right) = \delta^{(4)}\left(p_1 + p_2 - p_3 - p_4 - p'\right) \frac{\mathrm{d}p_3^3}{2E_3} \frac{\mathrm{d}p_4^3}{2E_4} \frac{\mathrm{d}p'^3}{2E'}\,, \tag{13}$$

$$\mathrm{d}PS_{n_\mathrm{f}-2}\left(s', m_{i_\mathrm{f}}^2, \ldots, m_n^2\right) = \delta^{(4)}\left(p' - \sum_{i=i_\mathrm{f}}^{n} p_i\right) \prod_{i=i_\mathrm{f}}^{n} \frac{\mathrm{d}p_i^3}{2E_i}\,, \quad \text{with } i_\mathrm{f} = 5\,. \tag{14}$$

In the c.m.s., Eq. (13) can be brought to the form of

$$\mathrm{d}PS_3\left(s, m_3^2, m_4^2, s'\right) = \frac{1}{8}\delta(\sqrt{s} - E_3 - E_4 - E') \frac{|\vec{p}_3||\vec{p}_4|}{E'} \mathrm{d}E_3 \mathrm{d}E_4 \mathrm{d}\Omega_3 \mathrm{d}\Omega_4\,, \tag{15}$$

with $E' = \sqrt{s' + (\vec{p}_3 + \vec{p}_4)^2}$. Introducing dimensionless variables $x = 2E_3/\sqrt{s}$ and $y = 2E_4/\sqrt{s}$, Eq. (15) can be written in the following way [17]:

$$\begin{aligned} \mathrm{d}PS_3\left(s, m_3^2, m_4^2, s'\right) &= \frac{1}{8} \frac{|\vec{p}_3||\vec{p}_4|}{2 - x + y\frac{|\vec{p}_3|}{|\vec{p}_4|}\cos\theta_{34}} \\ &\quad \times \mathrm{d}x\left[\delta(y - y_+) + \delta(y - y_-)\right] \mathrm{d}y \mathrm{d}\Omega_3 \mathrm{d}\Omega_4\,, \end{aligned} \tag{16}$$

where

$$\cos\theta_{34} = \cos\theta_3 \cos\theta_4 + \sin\theta_3 \sin\theta_4 \cos(\varphi_3 - \varphi_4) \tag{17}$$

and $y_\pm$ are the solutions, possibly 2, of the energy conservation equation, as described by the Dirac delta of Eq. (15)

$$\begin{aligned} \sqrt{s} - E_3 - E_4 - E' &= \sqrt{s} - \frac{\sqrt{s}}{2}x - \frac{\sqrt{s}}{2}y - \Bigg[s' + \frac{s}{4}x^2 - m_3^2 + \frac{s}{4}y^2 - m_4^2 \\ &\quad + 2\sqrt{\frac{s}{4}x^2 - m_3^2}\sqrt{\frac{s}{4}y^2 - m_4^2}\cos\theta_{34}\Bigg]^{1/2} = 0\,. \end{aligned} \tag{18}$$

The random variables of Eqs. (12) and (16) are generated in a similar way as described in [18] with only minor modifications, *i.e.*

— s' is generated according to $\sim 1/s'$ distribution.

— x is generated according to $\sim 1/(1-x)$ distribution.

— Azimuthal angles φ_3 and φ_4 are generated according to the uniform distribution.

— $\cos\theta_3 \in [-\cos\theta_{\rm cut}, \cos\theta_{\rm cut}]$ is generated according to $\sim 1/(1-\beta_3\cos\theta_3)$, with $\beta_3 = 2|\vec{p_1}||\vec{p_3}|/(2E_1E_3 - m_3^2)$.

— $\cos\theta_4 \in [-\cos\theta_{\rm cut}, \cos\theta_{\rm cut}]$ is generated according to $\sim 1/(a_4+\cos\theta_4)$, where

$$a_4 = \frac{2E_2\tilde{E}_4 - m_4^2}{2|\vec{p_2}|\sqrt{\tilde{E}_4^2 - m_4^2}} \tag{19}$$

and the meaning of $\tilde{E}_4$ is explained below.

— The $(n_{\rm f}-2)$-particle phase-space element of Eq. (14) is generated in a way similar to the s-channel phase-space generation of carlomat.

Note that energy E_4 of particle 4 is not known before $\cos\theta_4$ has been generated, $\cos\theta_{34}$ calculated according to Eq. (17) and Eq. (18) solved. Therefore, instead of E_4, we use in Eq. (19) $\tilde{E}_4$ being the solution of Eq. (18) for $\cos\theta_{34} = -1$, which corresponds to the collinear singularity being most pronounced. Then $\cos\theta_{34}$ is calculated according to Eq. (17) and substituted to Eq. (18). If there is no solution for y, then $\mathrm{d}^{3n_{\rm f}-4}$Lips of Eq. (12) is set to 0. If two solutions $y_\pm$ exist, then one of them is chosen randomly and the phase-space element $\mathrm{d}^{3n_{\rm f}-4}$Lips is multiplied by a factor 2.

4. Photon or gluon emission

Consider the reaction of the photon or gluon radiation of the following form:

$$1 + 2 \to 3 + 4 + \ldots + n + \gamma(p_\gamma)\,. \tag{20}$$

The phase-space element for the ISR is parameterized by

$$\mathrm{d}^{3(n_{\rm f}+1)-4}\mathrm{Lips} = \frac{1}{2}(2\pi)^{4-3(n_{\rm f}+1)} E_\gamma \mathrm{d}E_\gamma \mathrm{d}\Omega_\gamma \mathrm{d}PS_{n_{\rm f}}\left(s', m_3^2, \ldots, m_n^2\right)\,, \tag{21}$$

where E_γ and $\mathrm{d}\Omega_\gamma = \mathrm{d}\cos\theta_\gamma \mathrm{d}\varphi_\gamma$ are the energy and solid angle element of the photon in the c.m.s., respectively, $s' = (p_1 + p_2 - p_\gamma)^2 = s - 2\sqrt{s}E_\gamma$ is the reduced c.m.s. energy squared and $\mathrm{d}PS_{n_\mathrm{f}}(s', m_3^2, \ldots, m_n^2)$ is given by Eq. (14) with $i_\mathrm{f} = 3$.

The random variables of Eq. (21) are generated in the following way:

— E_γ is generated according to $\sim 1/E_\gamma$ distribution with the minimum photon energy E_γ^{cut}.

— $\cos\theta_\gamma \in [-\cos\theta_\gamma^{\mathrm{cut}}, \cos\theta_\gamma^{\mathrm{cut}}]$ is generated according to $\sim 1/(1-\beta^2\cos^2\theta_\gamma)$, with $\beta = \sqrt{1 - 4m_1^2/s}$ and, for the sake of simplicity, we have assumed equal masses of the initial-state particles.

— φ_γ is generated according to a uniform distribution.

— $\mathrm{d}PS_{n_\mathrm{f}}(s', m_3^2, \ldots, m_n^2)$ is again generated in a way that takes into account peaks due to the s-channel Feynman propagators.

The phase-space element for the FSR from either particle 3 or 4 of reaction (20) is written in the following way:

$$\begin{aligned}\mathrm{d}^{3n_\mathrm{f}-4}\mathrm{Lips} \;=\; & (2\pi)^{4-3n_\mathrm{f}} \mathrm{d}s' \mathrm{d}s'' \mathrm{d}PS_2\left(s, s', s''\right) \\ & \times \mathrm{d}PS_3\left(s', m_3^2, m_4^2, 0\right) \mathrm{d}PS_{n_\mathrm{f}-3}\left(s'', m_5^2, \ldots, m_n^2\right) \,, \end{aligned} \tag{22}$$

with $n_\mathrm{f} = n - 1$ and the 2-, 3- and $(n_\mathrm{f} - 3)$-particle phase-space elements defined appropriately according to Eqs. (13) and (14). The 3-particle phase-space element on the r.h.s. of Eq. (22), corresponding to the photon radiation off particle 3, is parameterized by

$$\mathrm{d}PS_3\left(s', m_3^2, m_4^2, 0\right) = \tfrac{1}{8}\mathrm{d}E_\gamma \mathrm{d}E_3 \mathrm{d}\cos\theta_3 \mathrm{d}\varphi_3 \mathrm{d}\varphi_{37} \,, \tag{23}$$

where the random variables are generated in the same way as in a program ee4fγ [19], *i.e.*

— E_γ is generated according to $\sim 1/E_\gamma$, with the minimum photon energy E_γ^{cut} boosted to the c.m.s. of particles 3, 4 and γ.

— E_3 is generated according to $\sim 1/(c_3 - E_3) \sim 1/(p_4 \cdot p_\gamma)$.

— $\cos\theta_3$, φ_3 and φ_{37} are generated according to the uniform distribution.

5. Quadruple precision

The multichannel probability distribution of Eq. (8) is in the current version of carlomat automatically supplemented with parameterizations (12), (21) and (22), which map away peaks due to t-channel Feynman propagators, or soft and collinear photon/gluon emission from the initial- or final-state particles. If the set of final-state four momenta of reactions (1), (11) or (20) is randomly generated according to the probability distribution $f_j(x)$, then normalization factors of all other distributions $f_i(x), i = 1, \ldots, N$ of Eq. (8) must be calculated for that particular set of four momenta in order to obtain proper phase-space normalization. This can be done also for the distribution $f_j(x)$ itself. In this way, we obtain a test of numerical stability of the kinematical part of the generated code. It is obvious that discrepancies between the normalization factor of $f_j(x)$ calculated from the random variables $x = (x_1, \ldots, x_{3n_f-4})$ and the normalization factor of $f_j(x)$ recalculated from the final-state four momenta indicate potential numerical instabilities in the phase-space calculation. The information about kinematical channels for which this test is not well-satisfied is recorded in the program output.

In the current version of carlomat, the problem is solved by the use of quadruple precision for the four momenta in kinematical routines and denominators of the Feynman propagators in the helicity amplitude calculation routines. However, then the MC program becomes much slower (by more than a factor 20).

6. Sample results

In Table I, we show the LO cross sections σ of the following reactions:

$$e^+e^- \to \mu^+\mu^-\tau^+\tau^- , \tag{24}$$

$$e^+e^- \to e^+e^-\mu^+\mu^- , \tag{25}$$

and the cross sections σ_γ of the corresponding radiative reactions with one photon in the final state at $\sqrt{s} = 200$ GeV and $\sqrt{s} = 500$ GeV. The complete results for reactions of the form of $e^+e^- \to 4f$, $4f\gamma$ are listed in [20]. As in [20], we impose the following cuts on angles and energies of the photon and final-state lepton:

$$\cos\theta(l, \text{beam}) \le 0.985 , \qquad \cos\theta(\gamma, \text{beam}) \le 0.985 , \quad \theta(\gamma, l) > 5^\circ ,$$
$$E_\gamma > 1 \text{ GeV} , \qquad E_l > 5 \text{ GeV} .$$

The first row, both for reaction (24) and (25), shows the results for σ and σ_γ of [20], while in the second and third row shown are the results obtained, respectively, with the double and quadruple precision MC code generated automatically with the current version of carlomat. Note that the

TABLE I

LO cross sections of $e^+e^- \to \mu^+\mu^-\tau^+\tau^-$ and $e^+e^- \to e^+e^-\mu^+\mu^-$, σ, and of the corresponding radiative reactions, σ_γ, at $\sqrt{s} = 200$ GeV and $\sqrt{s} = 500$ GeV with cuts given by (26). The first row for each channel shows the result of [20], while the second and third row are the results obtained, respectively, with the double and quadruple precision MC code generated automatically with the current version of carlomat.

Final state	$\sqrt{s} = 200$ GeV		$\sqrt{s} = 500$ GeV	
	σ [fb]	σ_γ [fb]	σ [fb]	σ_γ [fb]
$\mu^+\mu^-\tau^+\tau^-$	10.267(14)	2.1787(91)	2.5117(44)	0.6495(40)
	10.250(8)	2.1958(28)	2.4866(31)	0.6514(13)
	10.250(8)	2.1979(31)	2.4866(31)	0.6543(16)
$e^+e^-\mu^+\mu^-$	137.18(90)	12.93(31)	43.80(38)	4.58(12)
	137.52(75)	13.64(7)	42.14(32)	4.83(8)
	137.38(75)	13.67(7)	42.39(38)	4.91(4)

cross sections σ of reaction (24), where there are neither poles related to the t-channel Feynman propagator nor collinear photon emission, computed with the double and quadruple precision code are identical. However, there are some differences between the cross sections σ_γ of the radiative reaction (24) and cross sections of both the LO (σ) and radiative (σ_γ) reaction (25), where either the t-channel or collinear, or both kinds of poles are present at a time, computed with double or quadruple precision. Differences between the results of [20] and those of the present work can be traced back to the fact that the cross sections of [20] were obtained with a program ee4fγ, where the MC integration is performed in a single iteration, *i.e.* they are arithmetic means of all the calls to the integrand, while the current version of carlomat utilizes a multi-iteration approach with the results of iterations with smaller variance contributing more to the final result of the integration than those with the bigger variance.

7. Summary and outlook

The automatic generation of multichannel MC phase-space integration routines of carlomat, which up to now took into account only mappings of $\sim 1/s$ or the Breit–Wigner behaviour of the s-channel diagrams, is being supplemented with the parameterizations which map away the t-channel, soft and collinear photon or gluon emission. The quadruple precision versions of the routines for computation of the helicity amplitudes and phase-space parameterizations have been written. An upgraded version of carlomat including those improvements should be released soon, most probably in a few months.

REFERENCES

[1] G. Apollinari *et al.*, High-luminosity Large Hadron Collider HL-LHC, CERN Yellow Report, 2017, DOI:10.5170/CERN-2015-005.1 [arXiv:1705.08830 [physics.acc-ph]].

[2] A. Abada *et al.* [FCC Collaboration], *Eur. Phys. J. Spec. Top.* **228**, 1109 (2019).

[3] T. Behnke *et al.*, arXiv:1306.6327 [physics.acc-ph]; H. Baer *et al.*, arXiv:1306.6352 [hep-ph].

[4] M. Aicheler *et al.* (eds.), A Multi-TeV Linear Collider based on CLIC Technology: CLIC Conceptual Design Report, CERN Yellow Reports: Monographs, 2012, DOI:10.5170/CERN-2012-007; P. Roloff *et al.* [CLIC and CLICdp collaborations], arXiv:1812.07986 [hep-ex]; P.N. Burrows *et al.* [CLICdp and CLIC collaborations], The Compact Linear Collider (CLIC) — 2018 Summary Report, CERN Yellow Reports, 2018, DOI:10.23731/CYRM-2018-002 [arXiv:1812.06018 [physics.acc-ph]]; L. Linssen *et al.*, Physics and Detectors at CLIC: CLIC Conceptual Design Report (2012), DOI:10.5170/CERN-2012-003, arXiv:1202.5940 [physics.ins-det]]; T.K. Charles *et al.*, CLICdp, CLIC, The Compact Linear Collider (CLIC) — 2018 Summary Report, CERN Yellow Reports: Monographs, 2018, DOI:10.23731/CYRM-2018-002, arXiv:1812.06018 [physics.acc-ph]]; P. Roloff *et al.*, arXiv:1812.07986 [hep-ex].

[5] CEPC Study Group, arXiv:1809.00285 [physics.acc-ph]; arXiv:1811.10545 [physics.acc-ph].

[6] A. Abada *et al.* [FCC Collaboration], *Eur. Phys. J. C* **79**, 474 (2019); *Eur. Phys. J. Spec. Top.* **228**, 261 (2019); **228**, 755 (2019).

[7] PHOKHARA: http://ific.uv.es/~rodrigo/phokhara/; S. Tracz, H. Czyż, *Acta Phys. Pol. B* **44**, 2281 (2013).

[8] F. Jegerlehner, K. Kołodziej, *Eur. Phys. J. C* **77**, 254 (2017).

[9] A. Kanaki, C.G. Papadopoulos, *Comput. Phys. Commun.* **132**, 306 (2000); C.G. Papadopoulos, *Comput. Phys. Commun.* **137**, 247 (2001); C.G. Papadopoulos, M. Worek, *Eur. Phys. J. C* **50**, 843 (2007); A. Cafarella, C.G. Papadopoulos, M. Worek, *Comput. Phys. Commun.* **180**, 1941 (2009).

[10] F. Krauss, R. Kuhn, G. Soff, *J. High Energy Phys.* **0202**, 044 (2002); T. Gleisberg *et al.*, *J. High Energy Phys.* **0402**, 056 (2004); **0902**, 007 (2009).

[11] M. Moretti, T. Ohl, J. Reuter, arXiv:hep-ph/0102195; W. Kilian, T. Ohl, J. Reuter, *Eur. Phys. J. C* **71**, 1742 (2011).

[12] T. Stelzer, W.F. Long, *Comput. Phys. Commun.* **81**, 357 (1994); F. Maltoni, T. Stelzer, *J. High Energy Phys.* **0302**, 027 (2003).

[13] M.L. Mangano *et al.*, *J. High Energy Phys.* **0307**, 001 (2003).

[14] E. Boos *et al.*, *Nucl. Instrum. Methods Phys. Res. A* **534**, 250 (2004); A. Pukhov, arXiv:hep-ph/0412191.

[15] T. Gleisberg, S. Höche, *J. High Energy Phys.* **0812**, 039 (2008).

[16] K. Kołodziej, *Comput. Phys. Commun.* **180**, 1671 (2009); **185**, 323 (2014); **196**, 563 (2015); carlomat_3.1, `http://kk.us.edu.pl/carlomat.html`

[17] K. Kołodziej, M. Zrałek, *Phys. Rev. D* **43**, 3619 (1991).

[18] F.A. Berends, C.G. Papadopoulos, R. Pittau, *Comput. Phys. Commun.* **136**, 148 (2001).

[19] K. Kołodziej, F. Jegerlehner, *Comput. Phys. Commun.* **159**, 106 (2004).

[20] F. Jegerlehner, K. Kołodziej, *Eur. Phys. J. C* **23**, 463 (2002).